"CROSS-OVER" INFRARED SPECTROSCOPY: A VALUABLE TOOL FOR REMOTE SENSING OF OLIVINE PRESENCE AND COMPOSITION.

C. H. Kremer[1], J. F. Mustard[1], and C. M. Pieters[1], [1]Department of Earth, Environmental and Planetary Sciences, Brown University, Providence, RI (christopher_kremer@brown.edu).

Introduction: Visible and infrared spectroscopy have facilitated the remote detection of olivine on the Moon [e.g., 1,2], Mars [e.g., 3], and many asteroids [e.g., 4,5]. However, the chemical composition of olivine on planetary bodies remains only weakly constrained. Olivine comprises a solid solution series between forsterite (Mg_2SiO_4) and fayalite (Fe_2SiO_4), and the relative amount of Mg and Fe in olivine, referred to as Mg# (molar Mg/[Mg+Fe] x 100), commonly reflects the degree of magmatic differentiation of igneous rocks. Developing and validating a new technique for the remote sensing of olivine Mg-Fe composition would facilitate fundamental insights into planetary evolution.

Previous work [6] has shown that olivine exhibits two strong, distinctive spectral bands in the "cross-over" range of the infrared (here defined as 4-8 µm), between the visible-near infrared (VNIR, 0.5-3 µm) and mid-infrared (MIR, 8-15 µm) (Fig. 1). The positions of these bands at 5.6 and 6.0 µm apparently shift in position with respect to the Mg# of olivine, though this relationship remains largely unexplored.

We examined spectra measured from a suite of 52 olivine samples that span the Mg-Fe solid solution series in order to determine the potential applications of cross-over infrared spectroscopy to remote analysis of olivine composition. We investigated the relationship between olivine composition and the positions of the 5.6 and 6.0 µm bands by examining the reflectance and thermal emissivity spectra measured in the laboratory on a diverse suite of particulate olivine samples that span the full Mg-Fe solid solution series.

Background: Difficulties characterizing the chemistry of olivine arise in VNIR because variations in Mg-Fe content are expressed in the shapes and positions of three overlapping spectral bands near 1 µm [7]. Meanwhile, in the MIR, use of reststrahlen bands [8,9] for olivine composition is limited by their low spectral contrast in measurements of fine particulate materials, such as planetary regoliths [10]. The utility of mid-infrared features known as the Christiansen and transparency features is limited in spectra of mineral mixtures because signatures of other minerals may overwhelm signatures of olivine composition.

Meanwhile, the spectral character of olivine in the "cross-over" region has been mostly unexplored as a means to constrain the chemistry of solid-solution minerals, including olivine. The "cross-over" region spans the range of wavelengths in which silicate minerals transition between the body-scattering of photons in the VNIR and surface-scattering photons in the MIR. In the inner Solar System, the "cross-over" region also coincides with the transition between the dominance of solar photon reflection in the VNIR and thermal photon emission in the MIR. Among silicate minerals, bands in the 4-8 µm range arise as combinations and overtones of the fundamental vibration bands that occur at longer wavelengths in the MIR.
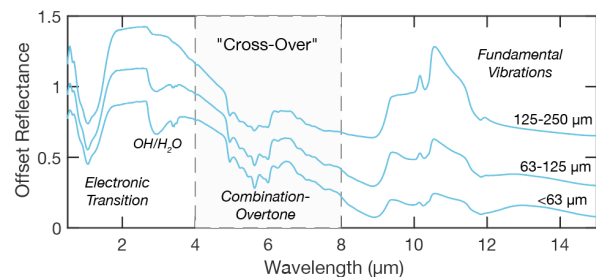

Figure 1. *Spectra of San Carlos olivine of varying grain size from the visible-near infrared to the mid-infrared. Physical origins of these bands are labeled.*

These overtone-combination bands include the 5.6 and 6.0 µm bands in olivine spectra, which are linked to the fundamental vibrational bands. While the 6.0 µm band in olivine may overlap with bands related to H_2O, pyroxene, and plagioclase, the 5.6 µm band evidently coincides with no observed bands in other major, rock-forming minerals [6]. The spectral contrast of the bands in the 4-8 µm region has been noted to increase with decreasing grain size, similar to the Christiansen feature but unlike the reststrahlen bands, making the "cross-over" region potentially attractive for remote studies of particulate materials on planetary surfaces.

Methods and Materials: The sample suite that we investigated included a total of 1) 27 samples of generally highly pure, synthetic olivine described by [11], 2) 16 samples of natural olivine separated from terrestrial rocks described by [12], 3) 6 samples of olivine or olivine-bearing samples from the Moon, and 4) 6 samples of olivine separated from Martian meteorites. Compositional data and sources for compositional data and spectra are detailed in [13]. Samples ranged in grain size from <60 to 250 µm, and the majority of samples had a grain size of <60 µm.

We compiled reflectance spectra measured in the NASA/Keck Reflectance Experiment Laboratory (RELAB) at Brown University [14] and the USGS Spectroscopy Library [15]. We compiled emission spectra from the University of Oxford's Planetary Analogue Surface Chamber for Asteroid and Lunar Environments [16] and the Arizona State University (ASU) Mars Space Flight Facility. All spectra were measured at a resolution of 4 cm^{-1} and sampling of 2 cm^{-1}.

We estimated the positions of the 5.6 and 6.0 μm bands first by visual inspection of spectra (see Fig. 2), without correcting for the slope of the spectral continuum (see Fig. 1 for shape of continuum). Although the 5.6 and 6.0 μm bands lie on a broad, negative spectral slope, both bands nevertheless each consist of a well-defined trough, allowing the positions of the band minima to be estimated and directly compared between samples. A band related to OH/H_2O at 3.0 μm appears in some spectra (see Fig. 1), but other features related to water, such as a 1.9 μm band, are absent from these spectra, indicating that water does not significantly interfere with band analysis of Fig. 2.
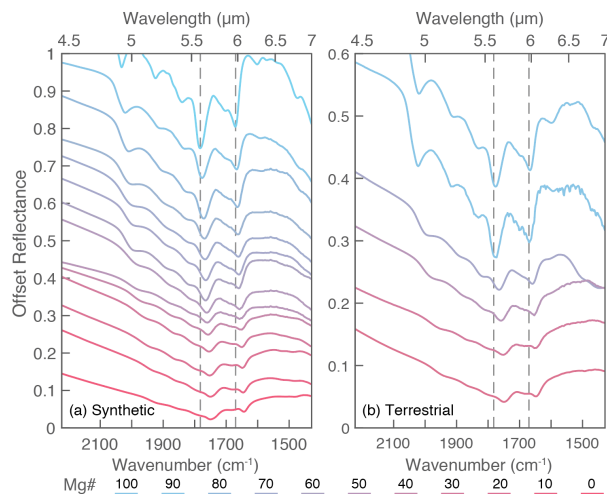

Figure 2. *Reflectance spectra of pure olivine samples. (a) Highly pure, synthetic olivine (SUNY suite) across the Mg-Fe solid solution series in the "cross-over" region. (b) Natural olivine derived from terrestrial rocks. These spectra are representative of other olivine samples in the studied suite. Decreasing Mg# ordered by color. Vertical lines highlight band trends. (see Fig. 3 for summary of band positions with other suites).*

Results: General trends in band position are visually evident in plots of spectra of the synthetic (Fig. 2a) and natural (Fig. 2b) olivine, and the trends in the positions of both bands for the entire sample suite are summarized in Fig. 3. We find that the wavelength positions of two discrete spectral bands at 5.6 and 6.0 μm shift systematically to longer wavelengths with

decreasing Mg#, with strong agreement among the trends in synthetic samples and natural terrestrial and extraterrestrial samples.

Across the full Mg-Fe solid solution series, the position of the 5.6 μm band shifts from 5.61 to 5.72 μm (1782 to 1747 cm^{-1}). The position of the 6.0 μm band shifts from 5.99 to 6.09 μm (1670 to 1643 cm^{-1}). Positions of the 5.6 and 6.0 μm bands in emission spectra (not shown) are similar to those in reflectance spectra of the same samples (Fig. 3). The 5.6 and 6.0 μm bands weaken somewhat with decreasing Mg# (Fig. 2).

Conclusion: This study indicates that band trends in olivine in the "cross-over" region are a highly promising means of constraining olivine composition remotely. In order to be used in the remote sensing of the Moon and other bodies, further work is needed to quantify these relationships and evaluate the spectral character of olivine in a lunar environmental context.
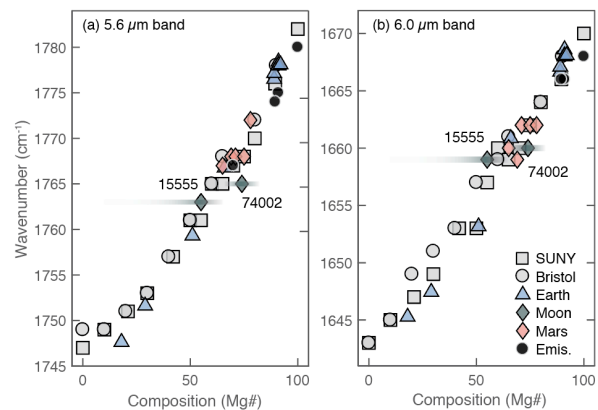

Figure 3. *Systematic trends in positions of (a) 5.6 and (b) 6.0 μm bands in reflectance spectra from entire olivine sample set (see examples in Figure 2), identified by sample suite. Positions of bands in emissivity spectra are shown as black circles. Band position data documented in [13].*

References: [1] Isaacson, P. J. et al. (2011) *JGR*, *116*, E00G11. [2] Yamamoto, S. et al. (2010) *Nature Geo*, *3*, 533–536. [3] Mustard, J. F. et al. (2005) *Science*, *307*, 1594–1597. [4] Reddy, V. et al. in: Michel, P. et al. (Eds.), *Asteroids IV*, University of Arizona Press, Tucson (2015). [5] Sunshine, J. M. et al. (2007) *M&PS*, *42*, 155–170. [6] Salisbury, J. W. *Remote Geochemical Analysis*, Cambridge University Press (1993), p. 594. [7] Sunshine, J. M. and Pieters, C. M. (1998) *JGR*, *103*, 13,675-13,688. [8] Hamilton, V. E. (2010) *Chemie der Erde*, *70*, 7–33. [9] Lane, M. D. et al. (2011) *JGR*, *116*, E08010. [10] Salisbury, J. W. et al. (1987) *JGR:SE*, *92*, 702–710. [11] Dyar, M. D. et al. (2009) *Am Min*, *94*, 883–898. [12] King, T. V. V. and Ridley, W. I. (1987) *JGR*, *92*, 11,457-11,469. [13] Kremer, C. H. et al. *GRL* (Submitted). [14] Pieters, C. M. and Hiroi, T. Houston, Texas (2004). [15] Kokaly, R. F. et al. *USGS Spectral Library Version 7*, USGS, Reston, VA, USA (2017). [16] Thomas, I. R. et al. (2012) *Review of Scientific Instruments*, *83*, 124502.